

SOME BASIC CONCEPTS OF WAVE-PARTICLE INTERACTIONS  
IN COLLISIONLESS PLASMAS

Bruce T. Tsurutani and Gurbax S. Lakhina  
Space Physics and Astrophysics Section  
Jet Propulsion Laboratory  
California Institute of Technology  
Pasadena, California 91109

## **ABSTRACT**

The physical concepts of wave-particle interactions in a collisionless plasma are developed from first principles. Using the Lorentz force, starting with the concepts of gyromotion, particle mirroring and the loss-cone, normal and anomalous cyclotron resonant interactions, pitch-angle scattering, and cross-field diffusion are developed. To aid the reader, graphic illustrations are provided,

## 1. INTRODUCTION

Wave-particle interactions play crucial roles in many phenomena occurring in the laboratory (Gill, 1981) and in space plasmas (Gary, 1992). In laboratory plasmas, wave-particle interactions come into play in several important applications like beat-wave acceleration, plasma heating using radio waves at ion and electron cyclotron frequencies, transport losses due to edge turbulence, etc. In space plasmas, wave-particle interactions are thought to be important for the formation of the magnetopause boundary layer, generation of outer zone chorus and plasmaspheric hiss emissions, precipitation of particles causing auroras, etc. Further, low-frequency waves can interact with charged particles over long spatial scale lengths and within the magnetosphere can transport energy from one region to another. For example, the interaction of ion cyclotron and whistler mode waves with Van Allen belt particles can scatter energetic protons and electrons into the loss cone, and thus lead to the ring-current decay within a magnetic storm recovery phase. Similarly, pitch angle scattering resulting from cyclotron resonance between an outer zone whistler mode chorus and 10- to 100-keV trapped substorm electrons can lead to the loss of electrons by precipitation. These precipitating electrons cause ionospheric phenomenon such as diffuse aurorae, enhanced ionization in the ionospheric D and E regions, and bremsstrahlung X-rays.

In space plasmas, the collision time between charged particles is generally very long compared to the characteristic time scales of the system, namely the inverse of the plasma frequency or cyclotron frequencies, etc., and therefore the plasma can be treated as collisionless. This would imply that there is virtually no dissipation in space plasmas, as particle-particle collisions are infrequent. This statement is correct provided there are no wave-particle interactions.

The presence of waves can introduce finite dissipation in a collisionless plasma. Charged particles are scattered by the wave fields, and the particles' momenta and energies change through this process. The interaction between a wave and a charged particle becomes strong when the streaming

velocity of the particle is such that the particle sees the Doppler-shifted wave frequency at its cyclotron frequency or its harmonics. This is the so-called cyclotron resonance interaction between the waves and particles. The special case of the Doppler-shifted wave frequency being zero (i.e., zero harmonics of the cyclotron frequency) corresponds to the well known Landau resonance. Landau (1946) showed that plasma waves in unmagnetized collisionless plasmas suffer damping due to wave-particle interactions, or “Landau damping”. The physical mechanism of Landau damping can be understood as follows: at Landau resonance, the particles do not see a rapidly fluctuating electric field of the wave, and hence can interact strongly with the wave. Those particles having velocities slightly less (greater) than the phase velocity of the wave are accelerated (decelerated) by the wave electric field to move with the wave phase velocity. Thus, the group of particles moving slightly slower (faster) than the phase velocity gain energy from (lose energy to) the wave. In a collisionless plasma characterized by a Maxwellian distribution function, the number of slower particles (in any interval around the phase velocity) are more than the number of faster particles, as shown in Figure 1a. Therefore, energy gained from the waves by slower particles is more than the energy given to the waves by faster particles, thus leading to net clamping of the waves. Consequently, Landau damping provides dissipation for a collisionless plasma. In a non-Maxwellian plasma, for example a beam-plasma system, one can create a situation where in a given velocity interval around the phase velocity of the wave, there are more faster particles than slower particles. Such a case is shown in Figure 1 b. This situation corresponds to inverse Landau damping or plasma (Cherenkov) instability, as the waves grow by gaining energy from the particles. For this situation we say that there is “free energy” available for wave growth. Similarly, the cyclotron resonant interactions between the waves and the particles give rise to a damping or instability phenomenon which is akin to Landau damping or instability [Stix, 1962].

Space plasmas are magnetized and can support a variety of plasma waves. The resonant interaction between electromagnetic waves and particles has been studied in detail [Kennel and Petschek, 1966, Lyons and Williams, 1984]. The interacting particles undergo pitch angle diffusion which

causes them to be precipitated in the atmospheric loss-cone or energy diffusion which results in a harder spectrum for the trapped particles.

In the review, we have tried to explain some fundamental concepts of wave-particle interactions involving electromagnetic waves. The Lorentz force plays a crucial role in the resonant interactions between electromagnetic waves and particles. Analytical expressions for pitch angle diffusion due to resonant wave-particle interactions are derived. We assume that the electron plasma frequency  $\Omega_{pe} = \sqrt{4\pi Nq^2/m}$  is greater than the electron cyclotron frequency,  $\Omega_e$ , where  $N$  is the electron number density and  $m$  is the electron mass.

## 2. BASIC CONCEPTS

Equation (1) is the Lorentz force in centimeter-gram-second (cgs) units. A particle with charge  $q$  moving with velocity  $\vec{V}$  across a magnetic field of strength  $\vec{B}_0$  experiences a force, the well known Lorentz force,  $\vec{F}_L$ , which is orthogonal to both  $\vec{V}$  and  $\vec{B}_0$ ,

$$\vec{F}_L = \frac{q}{c} \vec{V} \times \vec{B}_0, \quad (1)$$

where  $c$  is the speed of light. Figure 2 illustrates this situation for a positively charged particle (e.g., a proton) moving exactly perpendicular to a uniform magnetic field,  $\vec{B}_0$ . Since in a uniform field, the Lorentz force can change only the direction of the particle's velocity vector  $\vec{V}_\perp$  perpendicular to  $\vec{B}_0$ , the charged particle will exhibit a circular motion about the magnetic field  $\vec{B}_0$ . The radius of this orbit  $r$ , known as the particle gyroradius can be calculated by balancing the magnitude of the Lorentz force  $F_L = (qV_\perp B_0/c)$  with the centrifugal force  $mV_\perp^2/r$ , where  $m$  is the mass of the particle.

Equating these two forces and solving for  $r$ , one gets  $r = mV_{\perp}c/qB_0$ . Further, the angular frequency of motion  $d\theta/dt = Vi/r$  is equal to  $q B_0/mc$ , the cyclotron (or Larmor) frequency,  $\Omega$ , of the charged particle.

Figure 3 illustrates the concept of a particle pitch angle. For this particular example, we assume the particle charge is positive (positive ion). In a uniform magnetic field, the angle that the instantaneous particle velocity makes relative to the magnetic field vector is constant and is called the pitch angle. The particle velocity vector can be broken down into two orthogonal components, one parallel to  $B$ ,  $V_{\parallel}$ , and the other perpendicular to  $\vec{B}_0, \vec{V}_{\perp}$ , such that

$$\vec{V} = V_{\parallel} \vec{b} + \vec{V}_{\perp} \quad (2)$$

where  $\vec{b} = \vec{B}_0/B_0$ . The pitch angle,  $\alpha$ , of the particle is defined as  $\alpha = \sin^{-1}(V_{\perp}/V)$  as shown in Figure 3.

Since there are no forces exerted on the particle in the parallel direction in a uniform  $\vec{B}_0$ , the particle moves unimpeded with a constant velocity  $V_{\parallel}$  along  $\vec{B}_0$ . There is a cyclotron motion associated with the  $\vec{V}_{\perp}$  velocity component as shown above. Although the direction changes, the magnitude of  $\vec{V}_{\perp}$  remains unchanged. Thus, the pitch angle,  $\alpha$ , will be constant in a uniform  $\vec{B}_0$ . A positively charged particle thus moves in a left-hand spiral motion along the magnetic field. This handedness is important for resonant interactions, as we will illustrate later. Positive ions gyrate in a left-hand sense relative to  $\vec{B}_0$ , independent of whether they are moving along  $\vec{B}_0$  or antiparallel to  $\vec{B}_0$ . The central field line about which the particle gyrates in Figure 3, is called its guiding center. If the field oscillates slowly, the particle will follow accordingly.

Because electrons and negative ions have negative charge, the  $\vec{V} \times \mathbf{B}$  Lorentz force is oppositely directed to that of positively charged ions. Thus, electrons and negative ions gyrate about the magnetic field in a right-hand corkscrew sense, opposite to that shown in Figure 3.

If there is a strong magnetic field gradient, the particles can be “mirrored”, or reversed in direction by the Lorentz force. We show a particle at its mirror point in Figure 4 to illustrate this as a consequence of propagation in a non-uniform magnetic field. Although the Figure indicates a one dimensional gradient with a positive sense, i.e., the gradient of  $|\mathbf{B}|$  increasing to the right at the mirror point, the reader should imagine this to be a two-dimensional gradient where similar field line convergence occurs into and out of the paper as well. At the moment in time when the particle is being mirrored,  $V_{\parallel} = 0$ , and  $\vec{v} = \vec{v}_{\perp}$ , i.e., all of its velocity is in the perpendicular (to the field) plane. Due to the convergence of the magnetic field lines, the Lorentz force has a component toward the left, i.e., opposite to the mirror point, leading to particle acceleration in a direction opposite to the gradient, and thus “reflection”.

Since the Lorentz force operates in a direction orthogonal to the velocity vector, there is no work done. The total energy of the particle remains constant. Squaring equations (2) and multiplying by  $1/2 m$ , we get:

$$E_T = 1/2 mV^2 = 1/2 mV_{\parallel}^2 + 1/2 mV_{\perp}^2 = E_{\parallel} + E_{\perp} \quad (3)$$

where  $E_{\parallel}$  and  $E_{\perp}$  are the parallel and perpendicular kinetic energies of the charged particle. For a particle moving from left to right in a constant magnetic field,  $E_{\parallel}$  and  $E_{\perp}$  are each constant values. However, for a particle moving from left to right in a magnetic field gradient, as shown in Figure 4,  $E_{\parallel}$  decreases as  $E_{\perp}$  increases, keeping  $E_T$  constant. The mirror point is reached when  $E_{\parallel} = E_T$ . The particle then starts to move to the left with  $E_{\parallel}$  increasing (and  $E_{\perp}$  decreasing).

A magnetic “bottle” is depicted at the top of Figure 5. The magnetic field lines (flux) is pinched at two ends and expanded in the center. It has a positive gradient on the right (as one goes from left to right) and a negative gradient on the left. As a consequence, the Lorentz force at both mirror points is directed towards the center, i.e., away from both right and left mirror points. Particles with large pitch angles are “trapped” by the two mirror points and will bounce back and forth between them. However, particles that have  $0^\circ$  pitch angles or angles close to  $0^\circ$  will mirror at only extremely high field strengths and may escape out the ends of the “bottle”.

If one bends the lines of force, to a shape of a dipole field (Figure 5, bottom), we have the general shape of planetary magnetospheric fields. Particle radiation, such as the Van Allen radiation belts, are trapped on these field lines (Van Allen, 1991). The particles gyrate about the magnetic fields and also bounce back and forth between their mirror points. The particles also undergo a drift in the azimuthal direction around the Earth in the equatorial region due to the curvature and magnetic field gradients in the radial direction (this drift is not shown). Because the sense of drift is dependent on the sign of the charge on the particle, protons and electrons drift in opposite directions. These different drifts comprise a “ring of current” (ring-current) which intensifies during magnetic storms (due to injection and energization of ring-current particles). The injection of plasma causes decreases in the magnetic field measured at the Earth’s surface near the equator. This is called the storm main phase. The loss of these particles through wave-particle interactions and other processes (see Kozyra et al., 1997) leads to a decrease in the ring current and an increase in the field at the equator. This is called the storm recovery phase. It has been shown by Dessler and Parker (1959) and Sckopke (1966) that the magnitude of the field decrease in the main phase is directly related to the total energy of particles in the ring current.

How one gets energetic (energies - MeVs) particles on these trapped orbits is another problem. It is commonly believed that the neutrons produced during the interaction of cosmic ray particles with upper atmosphere atoms and molecules decay into protons and electrons within the magnetosphere thus populating the belts. These are called CRAND (cosmic ray albedo neutron decay) particles. Interaction of whistler waves with the energetic electrons may cause important losses of trapped electrons in the Van Allen belts (Tsurutani et al., 1975; Walt et al., 1996). Particles of lower energy (10 to 300 kV) can be also injected into the radiation belt by substorms and magnetic storm electric fields (Chen et al., 1997; Wolf, 1997). The losses of particles with magnetic storms are discussed by Sheldon and Hamilton (1993) and Kozyra et al. (1997).

The “loss cone” is the cone of pitch angles within which particles are lost to the upper atmosphere. The particle mirror points are deep in the atmosphere and the particles thus lose their energy by

collisions with atmospheric/ionospheric atoms and molecules and thus cannot return to the magnetosphere. Consequently, the magnetospheric equatorial phase space (pitch angle) distribution has signatures that look like Figure 6a. On the other hand, the precipitating particles, i.e., the particles which are scattered into the loss-cone, lose their energy to the neutral atoms and molecules. These atoms and molecules are excited to higher energy states, and produce auroral line and band emissions as they decay. This light is the aurora borealis (Northern hemisphere) and aurora australis (Southern hemisphere) (Figure 6b).

The size of the loss cone can be calculated by assuming constancy of the first adiabatic invariant  $\mu = E_{\perp}/B_0$ . This assumption is valid when the magnetic field changes slowly relative to the Larmor period and Larmor radius. For the dipole field shown in Figure 6b, we calculate the value below. As previously mentioned, at the mirror point, the particle's perpendicular kinetic energy  $E_{\perp}$  is equal to the total kinetic energy,  $E$ . Thus we can write  $\mu$  as  $E_{\perp}/B_{\text{Mirror}}$  at the mirror point. At the equator,  $\mu$  is equal to  $E_{\perp}/B_{\text{eq}}$ . Equating these two values we have  $E_{\perp}/B_{\text{Mirror}} = E_{\perp}/B_{\text{eq}}$ . We rearrange this as  $E_{\perp}/E_{\parallel} = B_{\text{eq}}/B_{\text{Mirror}}$ . From previous discussions, we know that  $E_{\perp}/E_{\parallel} = \frac{1}{2}mV_{\perp}^2 / \frac{1}{2}mV_{\parallel}^2 = \sin^2 \alpha_0$ , where  $\alpha_0$  is the particle pitch angle at the equator.

Thus, for the loss cone we have:

$$\sin^2 \alpha_0 = B_{\text{eq}}/B_{\text{Mirror}} \quad (4)$$

The values for  $B_{\text{eq}}$  and  $B_{\text{Mirror}}$  can be calculated assuming a dipole field dependence with distance,  $B/r^3 = \text{constant}$ . At the Earth, the surface equatorial field is approximately  $\sim 0.3$  Gauss. Thus for any dipole field line, the loss cone can be easily calculated. For any particle with pitch angles at the equator with  $\alpha < \alpha_0$ , such that the height of the mirror point is within the upper atmosphere, the particles are lost by collisions with neutrals. In the expression (4),  $\alpha_0$  is the pitch angle at the edge of the loss cone.

The Earth's field is not a pure dipole. There are variations in the local surface field strength. One area, called the Brazilian anomaly (previously called the South Atlantic Anomaly, but this magnetic

region has recently drifted inland) is a region of low magnetic field strength. In this region, the magnetic fields are weaker, and therefore the mirror points are shifted to lower altitudes. The particles which are normally just outside the loss cone will mirror deeper in the atmosphere than at other longitudes and are lost by collisions with the ionospheric/atmospheric atoms/molecules. A satellite passing just above the ionosphere would see more particle flux coming down (or higher radiation doses) as compared to the region outside the Brazilian anomaly.

### 3. Resonant wave-particle interactions

Previously, we showed that charged particles have a circular (cyclotron) motion about the ambient magnetic field (gyromotion) plus a translational motion along the magnetic field. When a particle senses an electromagnetic wave Doppler-shifted to its cyclotron frequency (or its harmonics), it can interact strongly with the waves. The condition for this cyclotron resonance between the waves and the particles can be written as:

$$\omega - \vec{k} \cdot \vec{V} = n\Omega \quad (5)$$

in expression (5),  $\omega$  and  $\vec{k}$  are the wave frequency (taken as positive here) and wave vector, and  $n$  is an integer equal to 0,  $\pm 1$ ,  $\pm 2$ , . . . . The case of  $n = 0$  corresponds to the Landau resonance discussed previously. When condition (5) is satisfied, the waves and particles remain in phase, leading to energy and momentum exchange between them.

For illustrative purposes, we first describe the  $n = 1$  (fundamental) resonance for electromagnetic waves propagating either parallel or anti-parallel to the magnetic field direction, i.e., we take  $\vec{k} = k_{\parallel} \vec{b}$ .

Thus (5) simplifies to:

$$\omega - k_{\parallel} V_{\parallel} = \Omega \quad (6)$$

If the frequency of the wave and the local gyrofrequency of the particle are known, then the particle resonance energy can be calculated. From (6) we have the parallel resonance speed,

$$V_{\parallel R} = \frac{(\omega - \Omega)}{k_{\parallel}}$$

Then, the parallel kinetic energy of resonant particles can be written as,

$$E_{\parallel R} = \frac{1}{2} m V_{\parallel R}^2 = \frac{1}{2} \frac{(\omega - \Omega)^2}{k_{\parallel}^2} = \frac{1}{2} m V_{ph}^2 (1 - \Omega/\omega)^2, \quad (7)$$

where  $V_{ph} = \omega/k_{\parallel}$  is the phase speed of the wave.

For the case in which the resonant waves are at frequencies much less than the ion cyclotron frequency, the wave-phase speed can be approximated by the local Alfvén speed  $V_A = [B^2/4\pi\rho]^{1/2}$ , where  $\rho$  is the ambient plasma mass density in cgs units.

Figure 7 illustrates the spatial variation of the wave (perturbation) magnetic vector as a function of distance along the magnetic field. Here we illustrate circularly-polarized, parallel-propagating electromagnetic waves. There are two basic types of polarization, right-handed and left-handed. Elliptical or linear polarizations are combinations of these two fundamental polarizations.

The polarization of waves is defined by the sense of rotation of the wave field with time at a fixed location. The sense is with respect to the ambient magnetic field and is independent of the direction of propagation.

In a magnetized plasma where  $\Omega_{pe} > \Omega^-$ , left-hand (polarized) waves can exist at frequencies up to the ion cyclotron frequency. At the high end of the frequency range, this mode is called an ion cyclotron wave. At low frequencies, this mode maps into the Alfvén mode branch. Right-hand waves can exist up to the electron cyclotron frequency. These waves are dispersive (in this case, higher frequencies have higher phase velocities as long as  $\omega$  is sufficiently below  $\Omega^-$ . As  $\omega$  approaches  $\Omega^-$ , the phase velocity decreases with increasing  $\omega$ , but the wave suffers heavy cyclotron damping and ceases to exist), and when they travel any substantial distance, the highest frequency component arrives first. Lightning-generated electromagnetic noise traveling within plasma “ducts” (field-aligned density enhancements or depletions with  $A_p/p \geq 5\%$ ) from one hemisphere to the other through the magnetosphere, end up having a whistling sound, thus the name “whistler mode”. The whistling sound starts at high frequencies and descends to lower frequencies. At low or MHD frequencies, this wave maps into the magnetosonic mode.

### 3.1 Normal Resonance

The normal cyclotron resonance between waves and charged particles is pictorially shown in Figure 8. For this resonant interaction, the waves and particles propagate towards each other. Left-hand positive ions interact with left-handed waves, and correspondingly right-hand electrons interact with right-hand waves. Since the waves and particles approach each other,  $\vec{k} \cdot \vec{V}$  has a negative sign. Thus the Doppler shift term  $(-\vec{k} \cdot \vec{V})$  in equation (5) is a positive one. The relative motion of the wave and particle causes Doppler-shift of the wave frequency,  $\omega$ , up to the particle cyclotron frequency,  $\Omega$ .

One plasma instability generating these waves in planetary magnetospheres is the “loss-cone instability”. This instability occurs when conditions  $T_{\perp}/T_{\parallel} > 1$  exist (Kennel and Petschek, 1966).  $T_{\parallel}(T_{\perp})$  is the ion or electron temperature parallel (perpendicular) to  $\vec{B}_0$ , assuming the plasma has a

“biMaxwellian” distribution. Electron loss cone instabilities generate whistler-mode emissions descriptively called aurora] zone “chorus” (Tsurutani and Smith, 1974, 1977; Kurth and Gurnett, 1991) and “plasmaspheric hiss” (Thorne et al., 1973; Tsurutani et al., 1975; Kurth and Gurnett, 1991) because of the sound they make when played through a loud speaker (the waves in the outer magnetosphere do not bounce several times like lightning whistlers, and frequency-time structures are due to intrinsic generation mechanisms).

Extremely low frequency (ELF) chorus is a common naturally-occurring, intense electromagnetic emission observed in the Earth’s magnetosphere [Russell et al., 1969, Dunckel and Hellwiel, 1969, Burton and Holzer, 1974; Burtis and Helliwell, 1976; Anderson and Maeda, 1977; Cornilleau-Wehrlin et al., 1978; Inan et al., 1983; Goldstein and Tsurutani, 1984, Alford et al., 1996].

The frequency-time characteristics of chorus can be banded and structureless, having falling tones and having “rising hook” emissions. Figure 9 shows an example of two-frequency rising-tone chorus detected by OGO-5 on August 15, 1968, at  $L = 5.9$  (for a dipole field, the  $L$  value is the distance in earth radius that the field line crosses the equatorial plane). This event had an average peak power of  $9 \times 10^{-7} \text{ (nT)}^2/\text{Hz}$ . One emission band is at  $-700 \text{ Hz}$ , the base frequency for tones rising from 700 to 1000 Hz, while a second thin band occurs at  $-1150 \text{ Hz}$  and consists of short  $\approx 0.1 \text{ s}$  duration dot-like emissions.

Chorus has been detected at all local times and at  $L$  values between the plasmapause and the magnetopause. However, it occurs predominantly between midnight and 1600 local time (LT). Chorus occurs principally in two magnetic latitude regions, namely, the equator (equatorial chorus), and at latitudes above  $15^\circ$  (high-latitude chorus) as shown schematically in Figure 10. The density of the dots indicates the regions where chorus is likely to be generated, the higher density indicating greater probability of generation. Equatorial chorus occurs primarily during

†

- substorms whereas the high-latitude chorus often occurs during quiet periods. Many observed features of equatorial chorus can be explained by the cyclotron resonance condition (eq. 5) between the whistler mode waves and energetic (10- to 100- keV) electrons injected by substorm electric fields. As seen from eqs. (6) - (7), for a particular frequency wave, the lowest velocity (or resonant energy) electron will be in cyclotron resonance at the equator where the gyrofrequency is minimum. Because the typical magnetospheric electron spectrum has more particles at lower energies, wave-particle interactions will be most intense at the equator, and this can lead to a rapid wave growth provided the energetic electrons have loss-cone distributions [Kennel and Petschek, 1966; Tsurutani and Smith 1977].

As energetic electrons continue convecting Earthward by substorm electric fields, the particle motion in the presence of magnetic field gradients and the magnetic field curvature causes the electrons to drift azimuthally toward dawn. This leads to energetic electron flux enhancement and precipitation principally in the post midnight sector. Due to compression of the dayside magnetosphere, the azimuthally drifting electrons end up on higher L values. This is the so-called drift shell splitting effect [Roederer, 1970]. This can explain the chorus asymmetry near midnight and the spread in L with local time.

There is an increase in chorus activity at dawn and the dawn-to-noon sector. Enhanced wave-particle interactions occur due to the lowering of resonant energies in the presence of increased ambient plasma density in those sectors. The latter effect is caused by ionospheric heating due to solar irradiation at these local times. Although energetic electrons continue to precipitate as the cloud drifts in longitude from midnight to dawn, the above effect leads to a remarkable increase in chorus intensity and electron precipitation between dawn and noon.

There is no single mechanism for the high latitude chorus. Some events appear to be generated by a loss cone instability. This local generation would occur in minimum B pockets which are regions

of local minimum magnetic field between 20° to 50° magnetic latitudes formed by the compression of the dayside magnetosphere [Roederer, 1970; Tsurutani and Smith, 1977]. Some other high-latitude chorus events appear to be equatorial chorus that has simply propagated to higher magnetic latitudes.

### 3.2 Anomalous Resonance

There is another type of resonance called anomalous cyclotron resonant interactions. This is shown for the case of positive ions in Figure 11. Positive ions interact with right-hand waves. They do so by overtaking the waves ( $V_{ii} > V_{ph}$ ) such that the ions sense the waves as left-hand polarized. Because the left-hand ion interacts with a right-hand wave, this interaction is called “anomalous”. From the expression in the resonance condition, the Doppler shift decreases the wave frequency to that of the cyclotron frequency. Examples of the instability generating such waves is the ion beam instability in planetary foreshocks (the magnetically connected region upstream of Shocks) [Hoppe et al., 1981; Smith et al., 1985; Goldstein et al., 1990; Gary, 1991; Verheest and Lakhina, 1993; Lakhina and Verheest, 1995], and ion pickup around comet [Tsurutani and Smith, 1986; Thorne and Tsurutani, 1987; Brinca, 1991; Tsurutani, 1991; Neubauer et al., 1993; Glassmeier et al., 1993; Mazelle et al., 1993]. The ion beam generates right-hand magnetosonic waves. In the foreshock case, the source of the ions is either shock-reflected (1-5 keV) solar wind particles or ions streaming from the magnetosheath with energies up to -40 keV. In the cometary case, neutral molecules/atoms sublime from the nucleus as the comet approaches the Sun. This neutral cloud can be  $\sim 10^7$  km in radius. The photoionization and charge exchange of cometary  $H_2O$  group neutrals ( $H_2O$ , OH, O) lead to the formation of a “beam” in the solar wind frame. For instability, the typical kinetic energy of the ions relative to the solar wind plasma is 30-60 keV,

The same anomalous cyclotron resonant interactions occur between electrons and left-hand mode waves. However, since the left-hand waves are at frequencies below the ion cyclotron frequency (a value far below the electron cyclotron frequency), resonant electrons are typically relativistic ( $E_{\parallel} > 1 \text{ MeV}$ ) for this interaction to take place. Even so, it is speculated that such an instability is occurring upstream of the Jovian magnetosphere perhaps due to leakage of Jovian radiation belt electrons (Smith et al., 1976; Goldstein et al., 1985).

The actual physical mechanism for particle pitch angle scattering due to electromagnetic waves is the Lorentz force. This is illustrated pictorially in Figure 12 for positive ions. At cyclotron resonance, the particle experiences the wave magnetic field  $\vec{B}$  gyrating in phase with the particle. For ease of visualization, we separate particle  $V$ , and  $V_{\parallel}$  components. Clearly the resonant interaction of particles with arbitrary pitch angles will be a combination of the two. In panel 12a), we show the case when the interaction is through  $V_{\perp}$ . Since a constant  $\vec{B}$  is imposed on the particle, the Lorentz force is in the  $\vec{B}_0$  direction. If the particle is propagating towards the right, the pitch angle will be decreased, and if the particle is traveling to the left, it will be increased. However, we have arbitrarily chosen the  $\vec{B}$  to be in the upward direction in the Figure. If the relative phase between the wave and particle were shifted by  $180^{\circ}$  such that  $\vec{B}$  was pointing downward, all of the results stated previously would be reversed.

Panel ( 12b) shows the particle interaction due to the parallel component of particle velocity. Here the Lorentz force is in a direction opposite to that of the gyromotion of the left-hand ion. Therefore, the interaction decreases  $V_{\perp}$ , ( $E_{\perp}$ ) and decreases the pitch angle of the particle. If the phase of the wave was different by  $180^{\circ}$ , such that  $\vec{B}$  was directed downward,  $\vec{F}_{\parallel}$  would accelerate the particle in  $E_{\parallel}$ , and the pitch angle would be increased.

Resonant wave-particle interactions occur on time scales small compared to the cyclotron period, thus the first adiabatic invariant  $\mu$  is not conserved (it is “broken”). In the inertial frame, the total

energy of the particle is not conserved during the wave-particle interaction, However, the energy of the particle in the rest frame of the wave is conserved as shown by the following physical argument, Let us assume that during wave particle interaction a particle gains a quantum of energy,  $\Delta E$  from a wave. Then  $\Delta E = h\omega/2\pi$ , where  $\omega$  is the wave frequency and  $h$  is the Planck's constant. The gain in the parallel momentum of the particle will be  $m\Delta V_{\parallel} = \frac{h k_{\parallel}}{2\pi \omega} \Delta E$ . If the energy gain is small compared to the total particle energy, then

$$\Delta E = m(V_{\parallel} \Delta V_{\parallel} + V_{\perp} \Delta V_{\perp}) = \frac{m\omega}{k_{\parallel}} \Delta V_{\parallel} = mV_{ph} \Delta V_{\parallel}, \quad (8)$$

where  $V_{ph} = \omega/k_{\parallel}$  is the phase velocity of the wave. Integrating equation (8), we get

$$\frac{1}{2} m V_{\perp}^2 + \frac{1}{2} m (V_{\parallel} - V_{ph})^2 = \text{constant}, \quad (9)$$

which shows that particle energy in the wave frame is conserved,

Equation (8) indicates that the particle energy changes, based on the sign of  $\Delta V_{\parallel}$  for a given phase velocity ( $V_{ph} > 0$  taken here). Particles that increase  $V_{\parallel}$  through resonant interactions increase energy and absorb wave energy, and those that decrease in  $V_{\parallel}$  lead to the generation of wave energy. The thermal background plasma which is out of resonance with the waves does not exchange energy during resonant wave particle interactions. In general, if one starts with a highly anisotropic pitch angle distribution (say  $T_{\perp} \gg T_{\parallel}$ ), one excites wave growth by the loss-cone instability. The waves in turn scatter the particles and "fill" the loss-cone to further reduce the free-energy available in the anisotropic pitch angle distribution until one gets to the stably trapped limit of Kennel and Petschek (1966).

For waves with electric field amplitudes,  $E$ , the particle's perpendicular kinetic energy increases or decreases depending on the phase of the wave with respect to the particle. The situation for increased  $E_{\perp}$  is shown in Figure 13. Analogous arguments can be made for wave-particle interactions due to electrostatic waves having a component  $\vec{E}$  perpendicular to  $\vec{B}_0$ , or the electric component of electromagnetic waves.

#### 4. Pitch Angle Scattering

The overall particle pitch angle scattering rates due to electromagnetic or electrostatic waves have been defined by Kennel and Petschek (1966), and have empirically been shown to be valid for the rate of scattering of electrons in the outer magnetosphere. Here we derive similar pitch angle scattering rates from simple physical arguments. We have  $\tan \alpha = V_{\perp}/V_{\parallel}$ , and for large pitch angle particles where  $V_{\perp} \cong V$ , we have

$$\Delta\alpha = -\Delta V_{\parallel} / V_{\perp} \quad (10)$$

The maximum change in the parallel velocity of a charged particle interacting with our electromagnetic wave is given by:

$$\Delta V_{\parallel} = \left( \frac{qV_{\perp}B}{m} \right) \Delta t$$

which with the help of (10) can be written as:

$$\Delta\alpha = \frac{eV_{\perp}}{mc} B \Delta t \frac{1}{V} = \frac{B}{B_0} \Omega \Delta t \quad (11)$$

The pitch angle diffusion rate is thus:

$$D \approx \frac{(\Delta\alpha)^2}{2\Delta t} \cong \frac{\Omega^2}{2} \left( \frac{B}{B_0} \right)^2 \Delta t \quad (12)$$

The time  $\Delta t$  is the time a particle  $k/2$  out of resonance changes its phase by one radian, or  $\Delta t \cong 2/\Delta k V_{\parallel}$ .

We now get:

$$D \approx \Omega \frac{B^*}{B_0} \frac{1/\Delta k}{V \cos \alpha} \frac{\Omega}{\cos \alpha} = \Omega \frac{B^2 / \Delta k}{B_0^2} \frac{k}{\cos \alpha} \quad (13)$$

Again, assuming large pitch angle particles,

$$D = \Omega \left( \frac{B}{B_0} \right)^2 \eta, \quad (14)$$

where  $\eta = (Q / \Delta k V_{\parallel})$  is the fractional amount of time that the particles are in resonance with the waves.

Particle transport across the magnetic field can be calculated once the mobility of the charged particles in the direction perpendicular to the ambient magnetic field, the so-called Pederson mobility, is known. The Pederson mobility,  $p_{\perp}$ , of particles in the direction perpendicular to  $\vec{B}_0$  (Schultz and Lanzerotti, 1974) is:

$$\mu_{\perp} = (c/B_0) \Omega \tau_{\text{eff}} / [1 + (\Omega \tau_{\text{eff}})^2] \quad (15)$$

In the above expression  $\tau_{\text{eff}}$  is the effective time between wave-particle “collisions”.

The maximum cross-field diffusion occurs when the particles are scattered at a rate equal to their gyrofrequencies, or  $\tau_{\text{eff}}^{-1} \approx eB_0/mc$  (Bohm diffusion). A spatial diffusion coefficient derived by Rose and Clark (1961) is:

$$D_{\perp} = \langle \Delta X_{\perp} \rangle^2 / 2\Delta\tau = \left( mV_{\perp}^2 / 2c \right) \mu_{\perp} \quad (16)$$

For Bohm (1949) diffusion,

$$D_{\perp} = E_{\perp} c / 2eB_0 = D_{\text{max}} \quad (17)$$

For conditions where  $\epsilon\tau_{\text{eff}} \gg 1$  and  $\tau_{\text{eff}} \approx 1/D$ , Tsurutani and Thorne (1982) have used equation (16) to determine the cross-field diffusion rate due to the magnetic component of electromagnetic waves by:

$$D_{\perp, B} = \frac{E_{\perp}}{e} \frac{c}{B_0} \frac{1}{\Omega\tau_{\text{eff}}} = 2(B/B_0)^2 D_{\text{max}} \quad (18)$$

Similarly for electrostatic waves, we get

$$D_{\perp, E} = 2(E/B_0)^2 (c/v)^2 D_{\text{max}} \quad (19)$$

Figure 14 shows the process of cross-field diffusion due to resonant wave-particle interactions.  $B_0$  is the original guiding center magnetic field line. After pitch angle scattering, the guiding center lies on the  $B'$  magnetic field line. The particle has “diffused” across magnetic field lines.

Using the measured wave amplitudes observed by ISEE 1 and 2 at the magnetopause, Thorne and Tsurutani (1991) showed, using expressions (18) and (19), that magnetosheath plasma can diffuse at one-tenth of the Bohm diffusion limit. This rate is adequate to account for the formation and maintenance of the magnetopause boundary layer.

### **FINAL COMMENTS**

We have tried to give simple explanations with illustrations to explain the fundamentals of wave-particle interactions. Clearly, more complex interactions and second-order effects which indeed are present, have not been included in this basic description.

### **ACKNOWLEDGMENTS**

B. T. Tsurutani wishes to thank Professor B. Buti for the invitation to lecture on the topic of wave-particle interactions at the Trieste, Italy Summer School, sponsored by UNESCO/Italy. He would like to particularly thank the Trieste Autumn College of Plasma Physics students, faculty members and visiting scholars for their enthusiastic reception of the talk form of this paper. Their kind encouragement led to the write-up of this paper. Portions of this work were performed at the Jet Propulsion Laboratory, California Institute of Technology, Pasadena under contract with the National Aeronautics and Space Administration. During the period Gurbax S. Lakhina held a Senior Resident Research Associateship of the National Research Council.

## References

- Bohm, D., Quantitative description of the arc plasma in a magnetic field, *Characteristics of Electrical Discharges in Magnetic Fields*, Ed. A. Guthrie and R. Walkerling, McGraw-Hill, New York 1, 1949.
- Alford, J., M, Engelbretson, R. Arnoldy, and U. Inan, Frequency variations of quasi-periodic ELF-VLF emissions: A possible new ground-based diagnostic of the outer high-latitude magnetosphere, *J. Geophys. Res.*, 101, 83, 1996.
- Anderson, R.R. and K. Maeda, VLF emissions associated with enhanced magnetospheric electrons, *J. Geophys. Res.*, 82, 135, 1977.
- Brinca, A.L., Cometary linear instabilities: From profusion to perspective, in *Cometary Plasma Processes*, ed. A. D. Johnstone, *Am. Geophys. Union, Geophysical Monograph 61*, 2 11, 1991.
- Burtis, W.J. and R.A. Helliwell, Magnetospheric chorus: Occurrence patterns and normalized frequency, *Planet. Space Sci.*, 24, 1007, 1976.
- Burton, R. K. and R. E. Holzer, The origin and propagation of chorus in the outer magnetosphere, *J. Geophys. Res.*, 79, 1014, 1974.
- Chen, M. W., M. Schulz and L.R. Lyons, Modeling of ring-current formation and decay: A review, to appear in *Magnetic Storms*, ed. by B .T. Tsurutani, Y. Kamide and W.D. Gonzalez, *Amer. Geophys. Un. Monograph*, 1997.
- Cornilleau-Wehrin, N., R. Gendrin, F. Lefeuvre, M. Parrot, R. Grard, D. Jones, A. Bahnsen, E. Ungstrup, and W. Gibbons, VLF electromagnetic waves observed onboard GEOS-1, *Space Sci. Rev.*, 22, 371, 1978.
- Dessler, A. J. and E. N. Parker, Hydromagnetic theory of magnetic storms, *J. Geophys. Res.*, 64, 2239, 1959.
- Dunckel, N., and R.A. Helliwell, Whistler mode emissions and the OGO satellite, *J. Geophys. Res.*, 74, 6371, 1969.

- Gary, S. P., Electromagnetic ion/ion instabilities and their consequences in space plasmas; A review, *Space Sci. Rev.* 56, 373, 1991.
- Gary, S. P., What is a plasma instability?, *EOS*, 7.?, 529, 1992.
- Gill, R. D., *Plasma Physics and Nuclear Fusion Research*, Acad. Press, London, 1981.
- Glassmeier, K.-H., U. Motschmann, C. Mazelle, F.M. Neubauer, K. Sauer, S.A. Fusilier, and M.H. Acuna, *J. Geophys. Res.*, 98, 20955, 1993.
- Goldstein, B.E. and B.T. Tsurutani, Wave normal directions of chorus near the equatorial source region, *J. Geophys. Res.*, 89, 2789, 1984.
- Goldstein, M. L., H. K. Wong, A.F. Vinas, and C. W. Smith, Large amplitude MHD waves upstream of the Jovian bow shock: Reinterpretation, *J. Geophys. Res.*, 90, 302, 1985.
- Goldstein, M. L., H. K. Wong, and K. M. Glassmeier, Generation of low frequency waves at comet Halley, *J. Geophys. Res.* 95, 947, 1990.
- Hoppe, M. M., C. 1'. Russell, L.A. Frank, T.E. Eastman, and E.W. Greenstadt, Upstream hydromagnetic waves and their association with backstreaming ion populations: ISEE 1 and 2 observations, *J. Geophys. Res.*, 86, 4471, 1981.
- Inan, U. S., R. A. Helliwell and W.S. Kurth, Terrestrial versus Jovian VLF chorus: A comparative study, *J. Geophys. Res.*, 88, 6171, 1983.
- Kennel, C. F. and H. E. Petschek, Limit on stably trapped particle fluxes, *J. Geophys. Res.*, 71, 1, 1966.
- Kozyra, J. U., V.K. Jordanova, R.B. Home and R.M. Thorne, Modeling of the contribution of electromagnetic ion cyclotron (EMIC) waves to storm time ring-current erosion, to appear in *Magnetic Storms*, ed. by B.T. Tsurutani, Y. Kamide and W. D. Gonzalez, *Amet. Geophys. Un. Monograph*, 1997.

- Kurth, W. S. and D.A. Gurnett, Plasma waves in planetary magnetospheres, *J.Geophys. Z/es.*, 96, 18977, 1991.
- Lakhina, G. S. and F. Verheest, Pickup proton cyclotron turbulence at comet P/Halley, *J. Geophys.Res.*, 100, 3449, 1995.
- Landau, L. P., On the vibrations of the electronic plasma, *J.Phys. (U.S.S.R.)*, 10, 25, 1946.
- Iyons, L. R. and D. J. Williams, *Quantitative Aspects of Magnetospheric Physics*, D. Reidel, Dordrecht, 1984.
- Mazelle, C. and F.M. Neubauer, Discrete wave packets at the proton cyclotron frequency at comet P/Halley, *Geophys.Res., Lett.*, 20, 153, 1993.
- Neubauer, F. M., K.-H., Glassmeier, A.J. Coates and A.D. Johnstone, Low-frequency electron plasma waves at comet P/Grigg-Skjellerup: Analysis and interpretation, *J.Geophys.Res.*, 98, 20937, 1993.
- Roederer, J. G., *Dynamics of Geomagnetically Trapped Radiation*, Springer, New York, 1970,
- Rose, D. J. and M. Clark, *Plasma and Controlled Fusion*, Wiley Cambridge, MA, 1961.
- Russell, C. T., R. E. Holzer, and E. J. Smith, OGO 3 Observations of ELF noise in the magnetosphere, 1. Spatial extent and frequency of occurrence, *J.Geophys.*, 74, 755, 1969.
- Schulz, M. and L. J. Lanzerotti, *Particle Diffusion in the Radiation Belts*, Springer-Verlag, New York, 1974.
- Sckopke, N., A general relation between the energy of trapped particles and the disturbance field near the Earth, *J.Geophys. Res.*, 71, 3125, 1966.
- Sheldon, R.B. and D.C. Hamilton, Ion transport and loss in the Earth's quiet ring-current: 1. Data and standard model, *J.Geophys. Res.*, 98, 13491, 1993.
- Stix, T. M., *The Theory of Plasma Waves*, McGraw Hill, New York, 1962.

- Smith, C. W., M. L. Goldstein, S. P. Gary, and C.T.Russell, Beam driven ion cyclotron harmonic resonance in the terrestrial foreshock, *J.Geophys.Res.*, 90, 1929, 1985.
- Smith, E. J., B. T. Tsurutani, D. L. Chenette, T.F.Conlon, and J.A. Simpson, Jovian electrons: Correlation with the interplanetary field direction and hydromagnetic waves, *J.Geophys. Res.*, 81, 65, 1976.
- Thorne, R. M., E.J. Smith, R.K. Burton, and R.E.Holzer, Plasmaspheric hiss, *J.Geophys. Res.*, 76, 1581, 1973.
- Thorne, R. M., and B. T. Tsurutani, Wave-particle interaction in the magnetosphere boundary layer, in *Physics of Space Plasmas*, SPI Conference Proceedings and Reprint Series, Number 10, Scientific Publishers, Inc., Cambridge, MA, 119, 1991.
- Tsurutani, B. T., and E. J. Smith, Postmidnight chorus: A substorm phenomenon, *J.Geophys. Res.* 79, 118, 1974.
- Tsurutani, B. T., E. J. Smith, and R.M.Thorne, Electromagnetic hiss and relativistic electron losses in the inner zone, *J.Geophys.Res.*, 80, 600, 1975.
- Tsurutani, B. T. and E. J. Smith, Two types of magnetospheric ELF chorus and their substorm dependence, *J. Geophys. Res.* 6'2, 5112, 1977.
- Tsurutani, B.T. and E.J.Smith, Hydromagnetic waves and instabilities associated with cometary ion pickup: ICEE observations, *Geophys Res. Lett.*, 13, 263, 1986.
- Tsurutani, B. T., Comets: A laboratory for plasma waves and instabilities, in *Cometary Plasma Processes*, ed. A. D. John stone, Am. Geophys. Union, *Geophysical Monograph* 61, 189, 1991.
- Tsurutani, B. T. and R. M. Thorne, Diffusion processes in the magnetopause boundary layer, *Geophys. Res. Lett.*, 9, 1247, 1982.
- Van Allen, J. A., Why radiation belts exist, *EOS*, 72, 361, 1991.

•  
Verheest, F., and G. S. Lakhina, Resonant electromagnetic ion/ion beam turbulence at comet P. Grigg-Skjellerup, *J. Geophys. Res.*, %S, 21017, 1993.

Walt, M., U.S. Inan, and H. D. Voss, Trapped electron losses by interactions with coherent VLF waves, in *Workshop on the Earth's Trapped Particle Environment*, ed, G. D. Reeves, AIP Conference proceedings 383, Am, inst. Phys., New York, 65, 1996.

Wolf, R, A., Modeling convection effects in magnetic storms, to appear in *Magnetic Storms*, ed. by B. T., Tsurutani, Y. Kamide and W.D. Gonzalez, *Amer. Geophys. Un. Monograph*, 1997.

## FIGURE CAPTIONS

Figure 1. A schematic of a group of particles interacting resonantly with waves in an unmagnetized plasma. Case a) corresponds to a Maxwellian plasma. The energy gained from the waves by the slower particles is more than the energy given to the waves by the faster particles. Case b) corresponds to a beam-plasma system where the phase velocity of the wave is less than the beam speed  $V_0$ .

Figure 2. The Lorentz force and a positively charged particle gyromotion in a uniform magnetic field.

Figure 3. The “pitch” angle of a positively charged particle.

Figure 4. A schematic illustrating the mirror force.

Figure 5. Magnetic bottles for plasma particles.

Figure 6. The equatorial loss cone (a), and auroras associated with particle pitch angle scattering into the loss cone (b).

Figure 7. Left-hand and right-hand parallel propagating circularly polarized electromagnetic waves.

Figure 8. Normal first-order cyclotron resonance between electromagnetic circularly polarized waves and charged particles.

Figure 9. Two-frequency rising tone chorus. One emission band is at  $\sim 700$  Hz, the base frequency for chorus rising from 700 to 100 Hz, and a second band at  $\sim 1150$  Hz, consisting of  $\sim 0.1$ s duration dotlike emissions. In the blown-up part of the figure, the higher-frequency dots are seen to be the high-frequency portions of the rising tones with a strong extinction in the frequency range from 1000 to 1100 Hz ( $\sim 0.5\Omega$ ). Taken from Tsurutani and Smith (1974).

Figure 10. A schematic representation of the regions in which chorus is generated. The figure shows the magnetic field in the noon-midnight meridian plane based on the magnetosphere

field model of Mead and Fairfield [ 1975]. The regions in which chorus is thought to be produced are noted by dots. Near midnight, chorus is generated close to the magnetic equator by substorm-injected electrons from the plasmashet. Chorus continues to be generated near the magnetic equator as the electrons drift around from dawn to noon. On the dayside at large L values, chorus is also generated over a much larger span of magnetic latitudes. Within 1-2  $R_E$  of the magnetopause, chorus may originate in minimum B pockets, which are local regions of minimum magnetic field strength that occur at high latitudes as a result of the solar wind compression of the dayside magnetosphere (taken from Tsurutani and Smith, 1979).

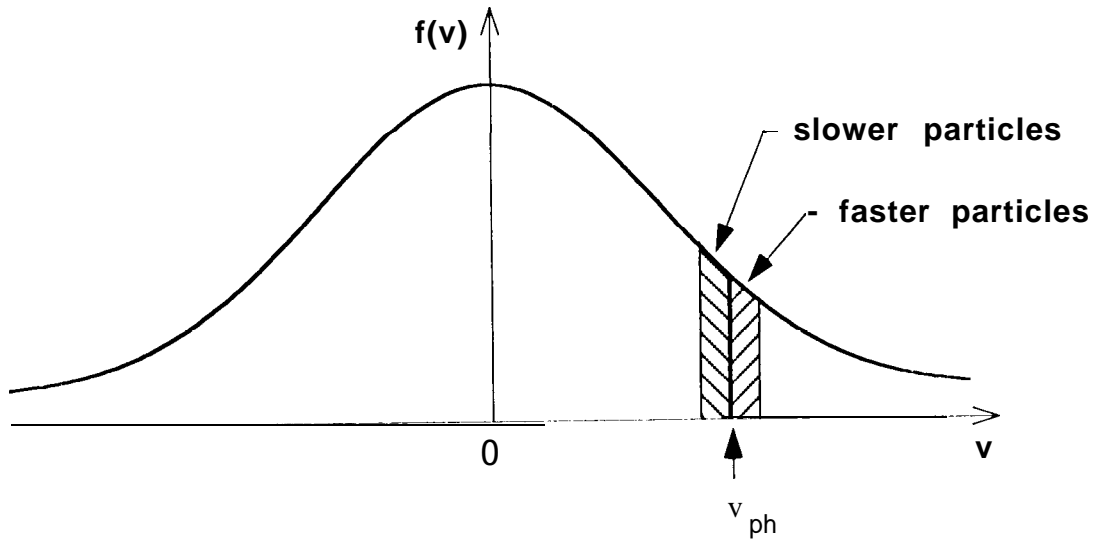
Figure 11. A schematic illustrating anomalous cyclotron resonance between electromagnetic circularly polarized waves and positively charged particles.

Figure 12. Pitch angle scattering by resonant electromagnetic waves.

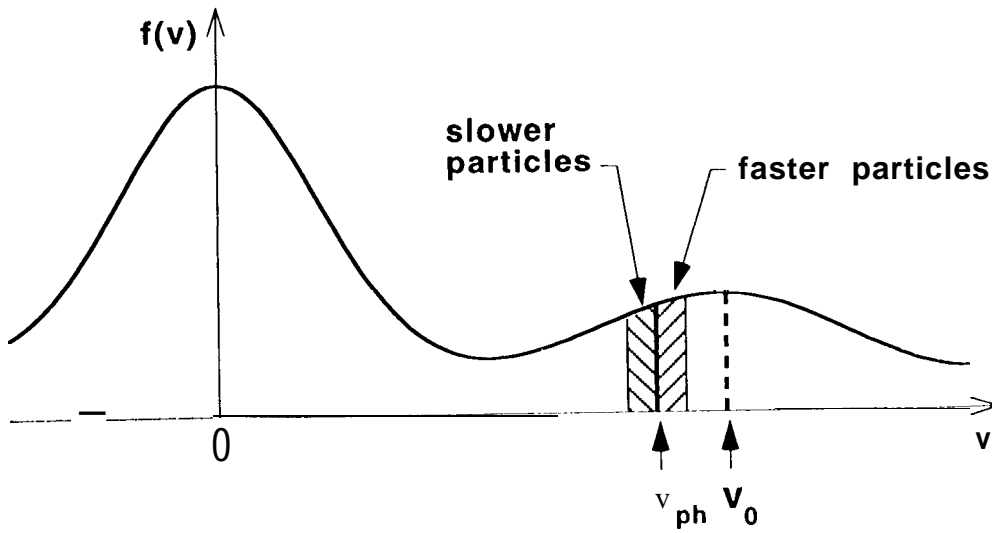
Figure 13. Pitch angle scattering by the electric component of resonant electromagnetic or electrostatic waves.

Figure 14. Particle cross-field diffusion by resonant interactions with waves,



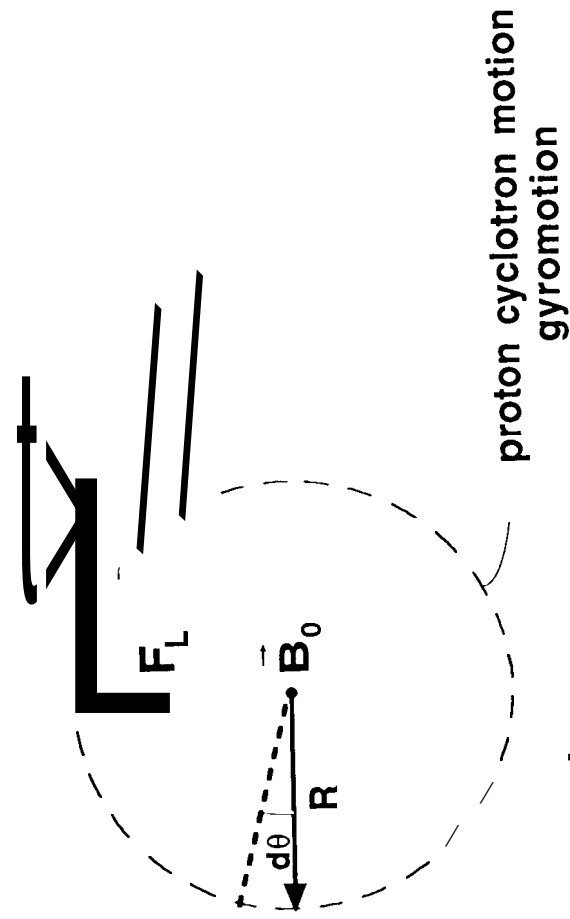
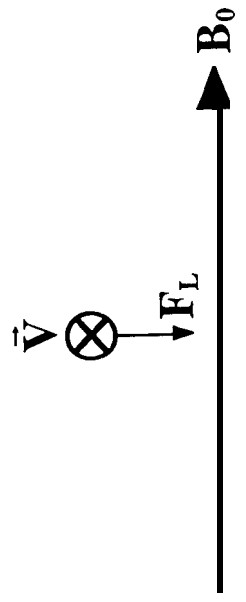
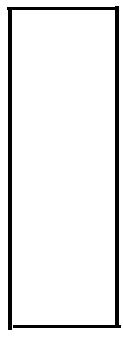


a)



b)

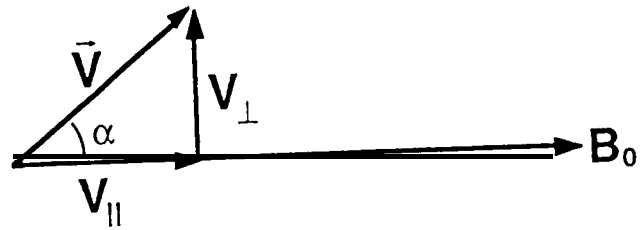
# Lorentz Force



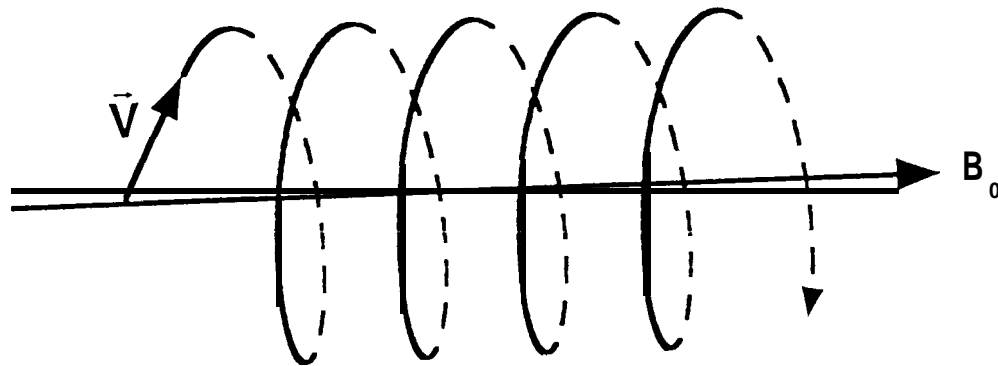
Left hand rotation

Figure 2

## Pitch Angle $\alpha$



$$\sin \alpha = \frac{v_{\perp}}{v}$$

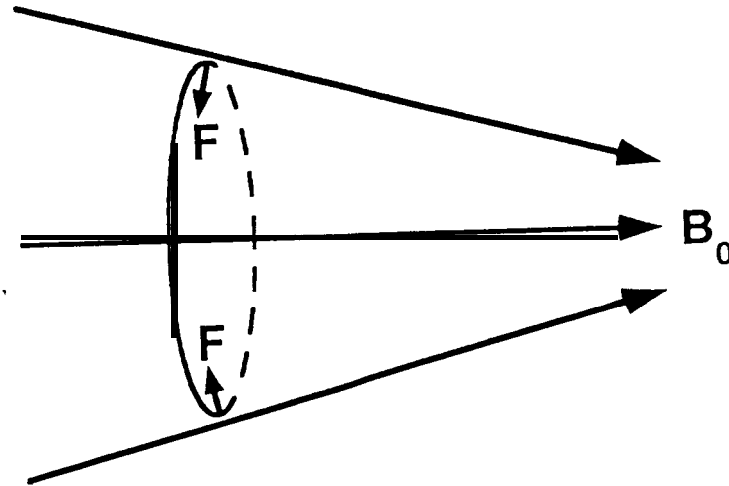


Left hand corkscrew  
motion spiral

Figure

A.3

## Mirror Force



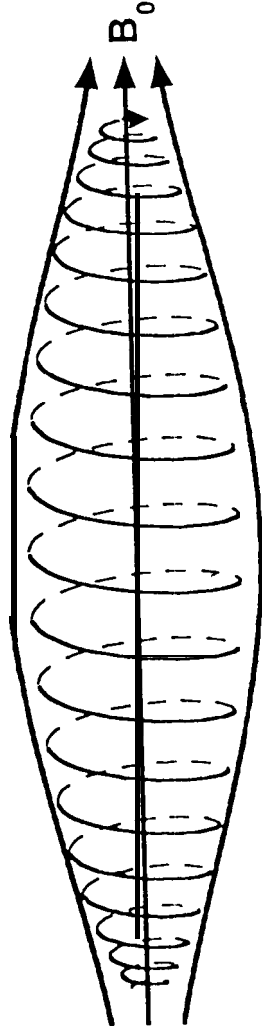
Lorentz force is  $\perp$  to  $\vec{V}$ , so it does no work.

$$\vec{V} = \vec{V}_{\parallel} + \vec{V}_{\perp}$$

$$\frac{1}{2} m |\vec{V}|^2 = \frac{1}{2} m V_{\parallel}^2 + \frac{1}{2} m V_{\perp}^2 = E_{\parallel} + E_{\perp} = E_{\text{total}}$$

mirroring transforms parallel energy into perpendicular energy with  $E_{\text{total}}$  conserved

# Magnetic Bottle



$$\mu = \frac{E_{\perp}}{B} = \text{constant}$$

(first adiabatic invariant)

# Earth's Radiation Belts

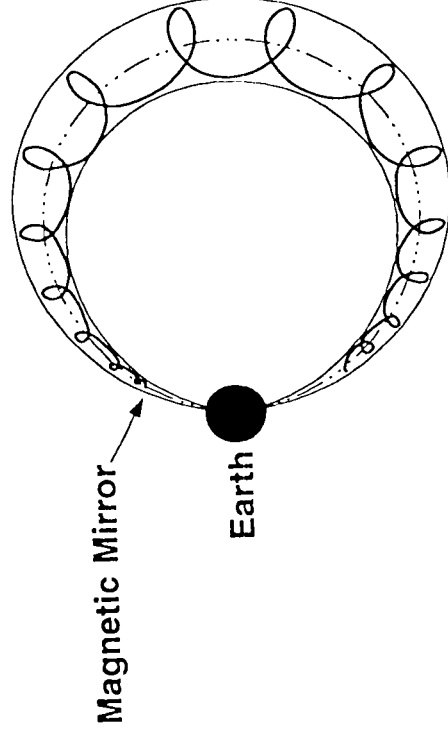
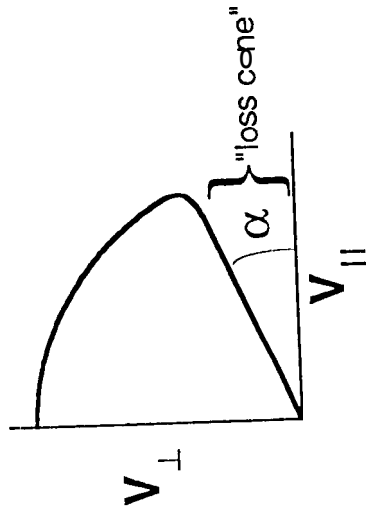


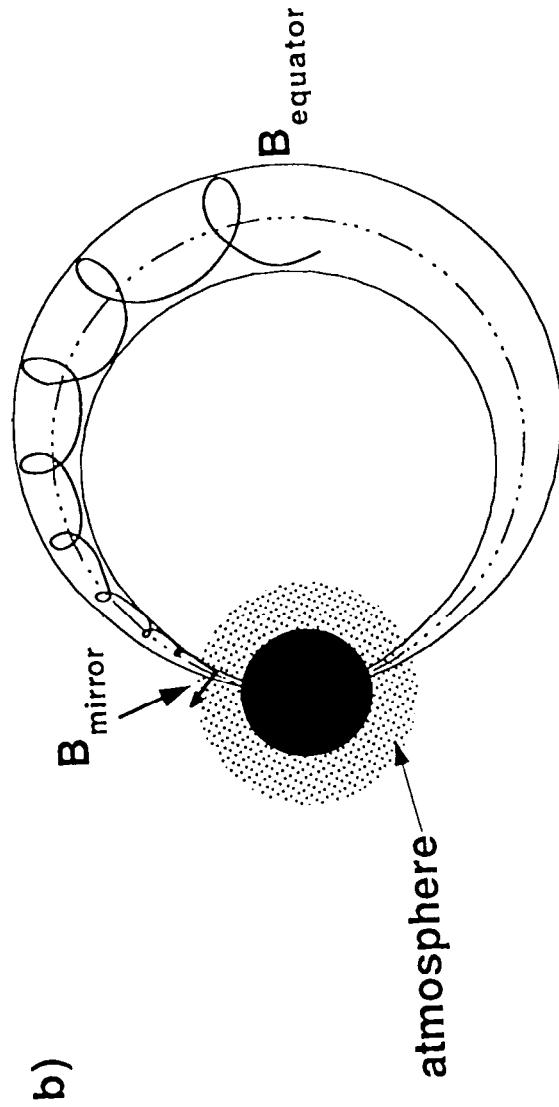
Figure 5

# Loss Cone



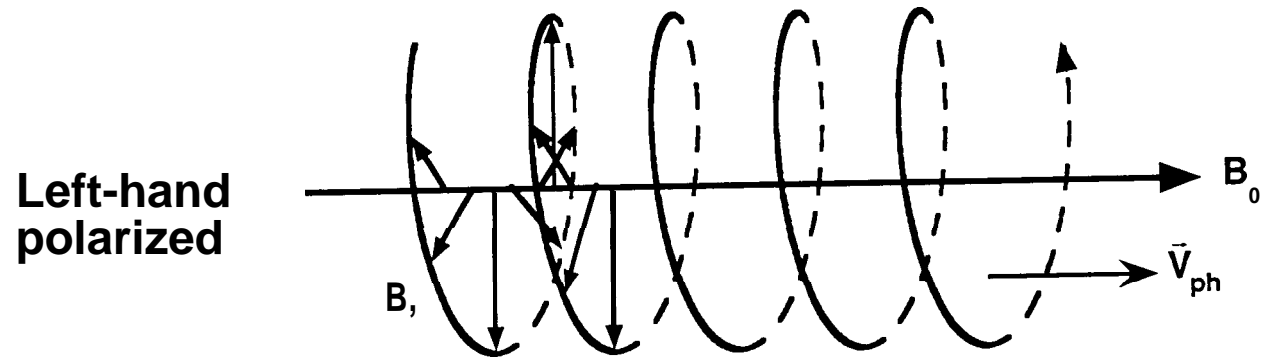
a)

# Aurora Borealis and Australis

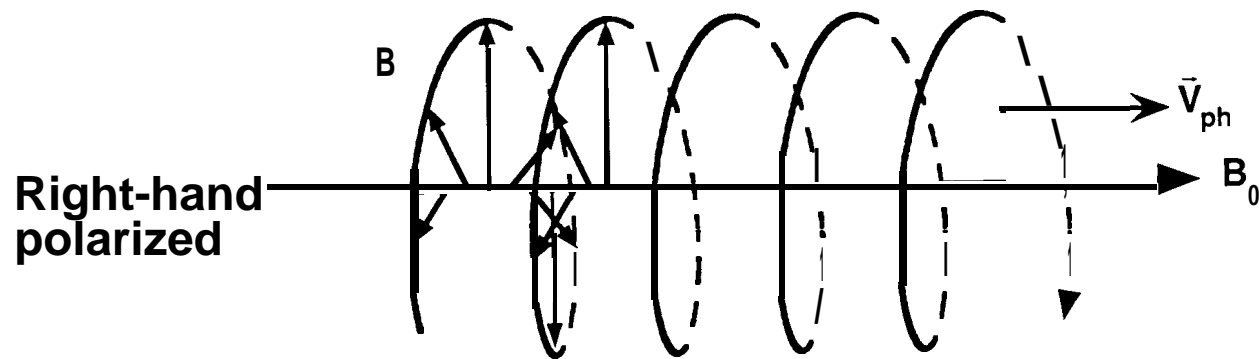


b)

# Electromagnetic Wave Polarizations

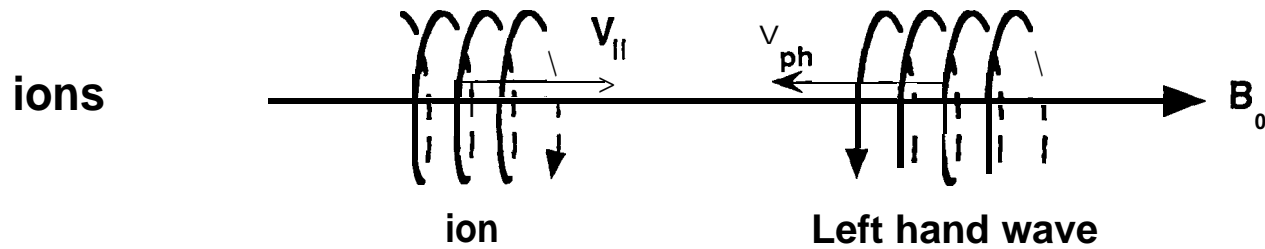


**ion cyclotron (high  $\omega$ )**  
**Alfvén mode (low  $\omega$ )**



**whistler mode (high  $\omega$ )**  
**magnetosonic mode (low  $\omega$ )**

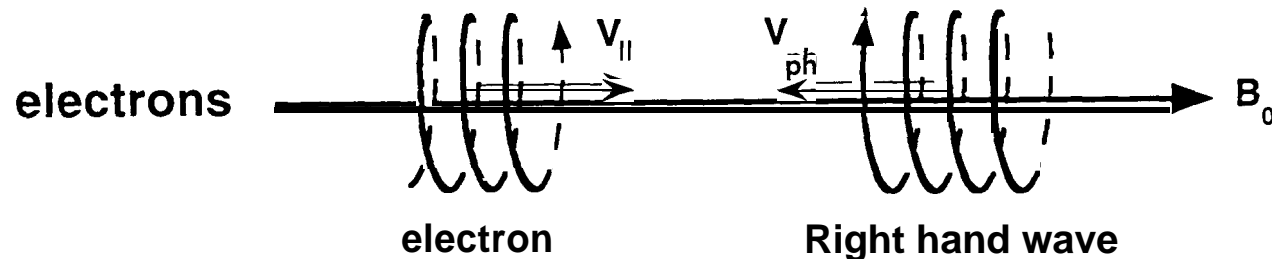
## (Normal) Cyclotron Resonance



$$\omega - \vec{k} \cdot \vec{V} = \Omega^+$$

$$\omega + k_{||} V_{||} = \Omega^+$$

The relative motion between the wave and particle Doppler shifts the wave up to the ion cyclotron frequency.



$$\omega + k_{||} V_{||} = \Omega$$

Figure, 8

OGO-5 REV 63  
15 AUGUST, 1968  
0118 LOCAL TIME

MLAT =  $-4.2^\circ$   
L =  $5.92 R_e$   
 $B_0 = 937^e$

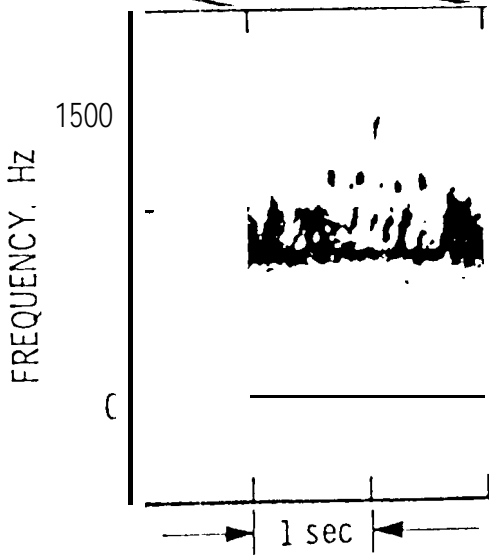
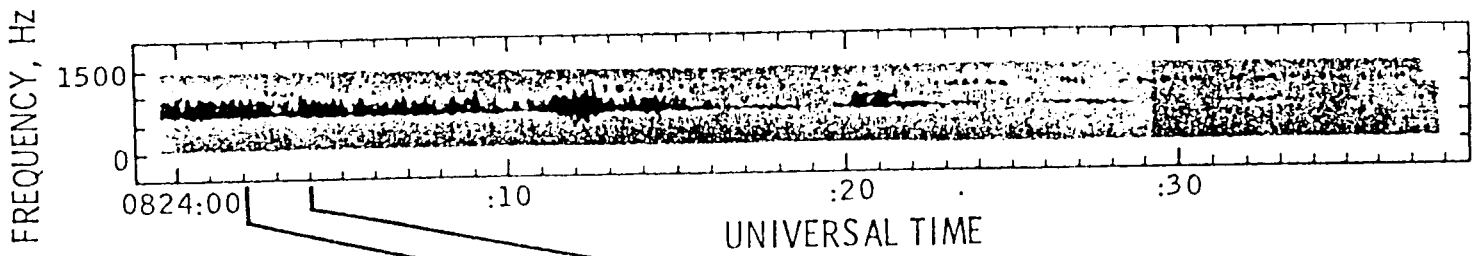
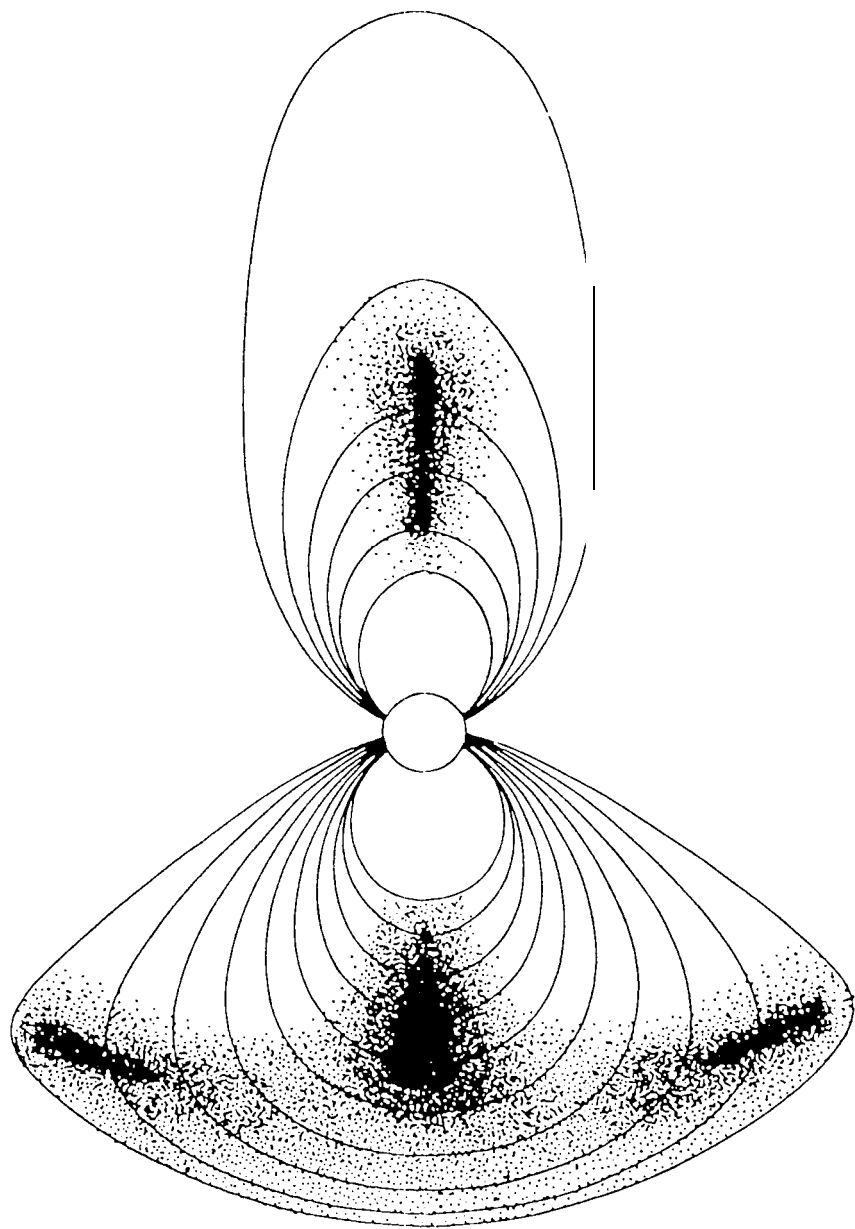
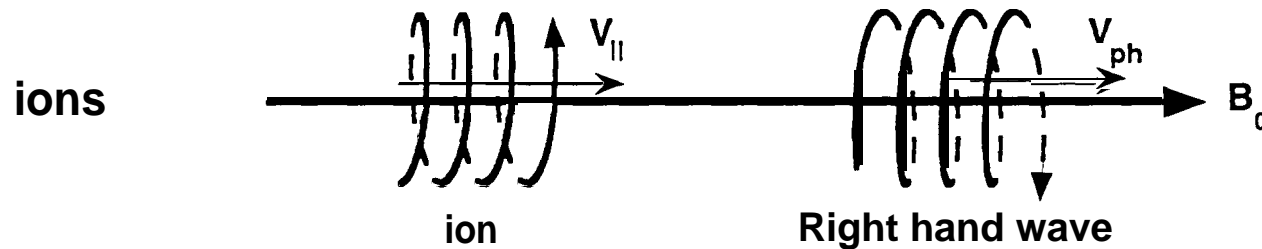


Figure 2



# Anomalous Cyclotron Resonance

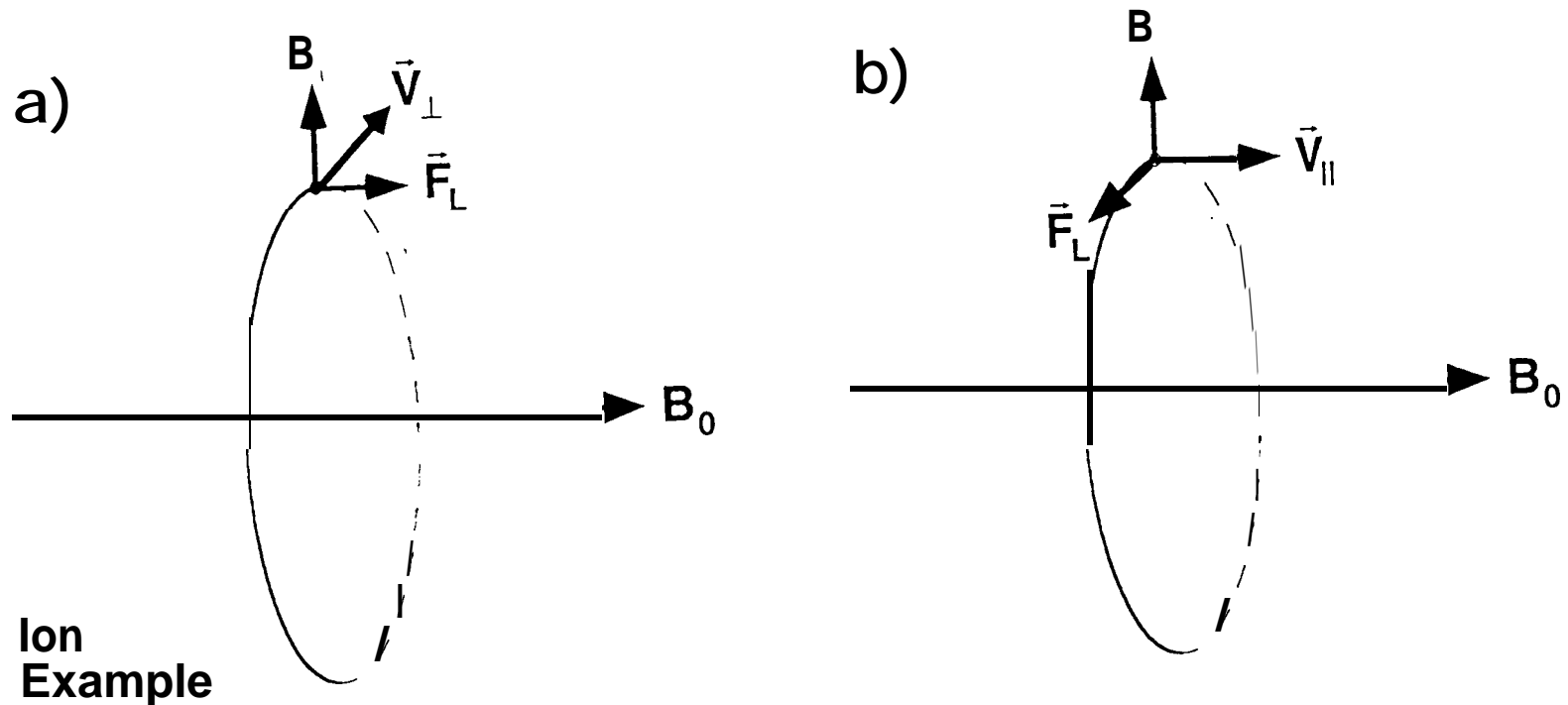


The left hand ion overtakes the right hand wave ( $v_{||} > v_{ph}$ ) and senses it as left hand polarized.

$$\omega - k_{||} v_{||} = -\Omega^+$$

Note that the relative motion between the particle and wave Doppler shifts the wave down to the gyrofrequency. The interaction is “anomalous” because right hand waves interact with left hand ions.

# Wave-Particle (Cyclotron) Interaction



The  $\mathbf{V} \times \mathbf{B}$  interaction with the wave  $\mathbf{B}$  increases, or decreases the parallel velocity of the particle depending on particle direction of propagation.

9

Figure,

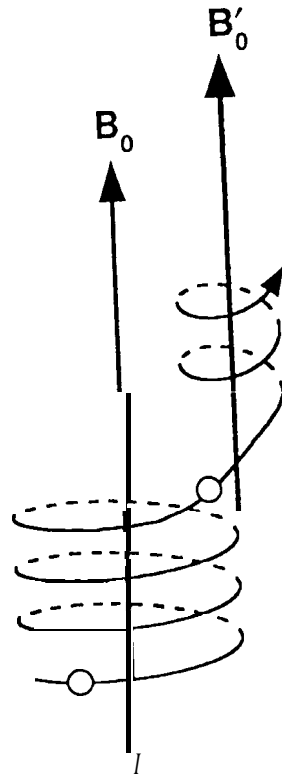


Figure 14

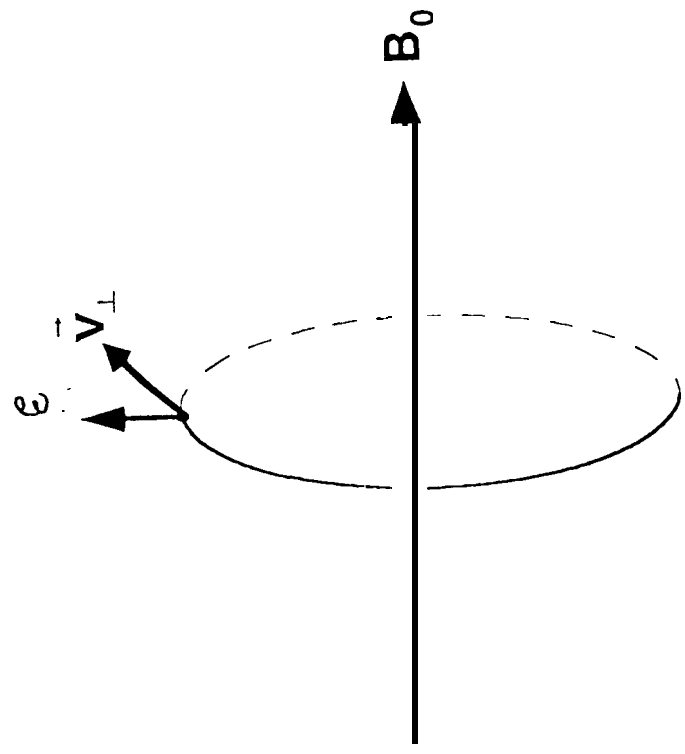


Figure 3  $\Sigma$